Electronic Supplementary Material

Facile assembly of nanosheet array-like CuMgAl-layered double hydroxide/rGO nanohybrids for highly efficient reduction of 4-nitrophenol

Liguang Dou and Hui Zhang*

State Key Laboratory of Chemical Resource Engineering, Beijing University of Chemical Technology, Beijing 100029, China.

*Correspondence should be addressed to Hui Zhang.
E-mail: Huizhang67@gst21.com
Tel.: +8610 64425872
Fax: +8610 64425385

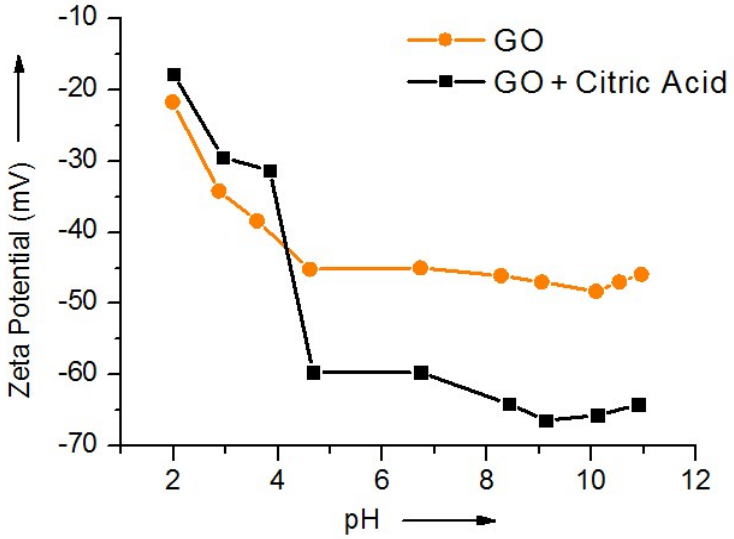

Figure S1. Zeta potential profiles of a GO dispersion (~0.05 mg/mL) before and after addition of citric acid (~0.2 mg/mL) as a function of pH values in aqueous dispersion.

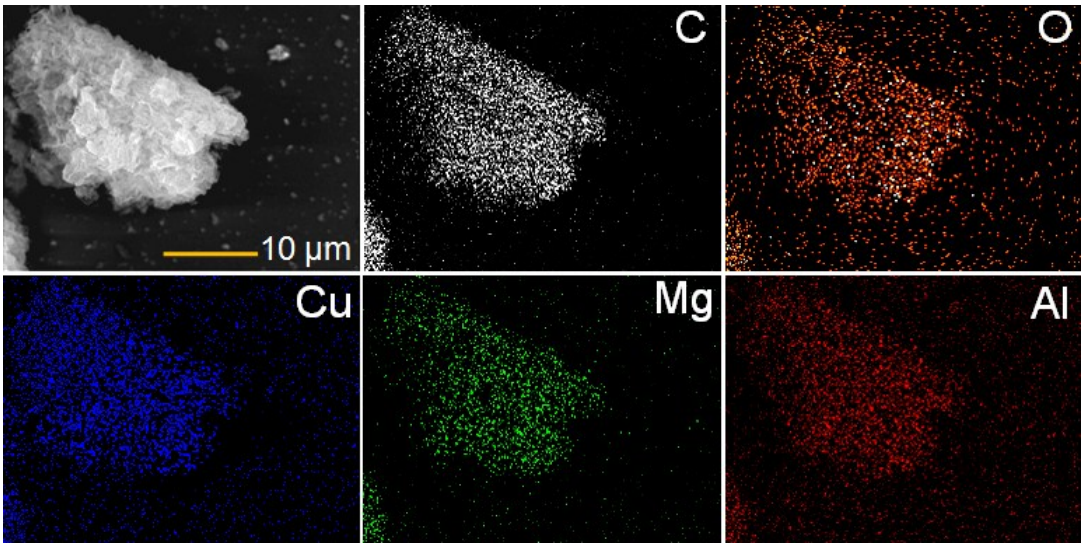

Figure S2. EDS mapping analyses of the nanohybrid 1.0Cu-LDH/rGO.

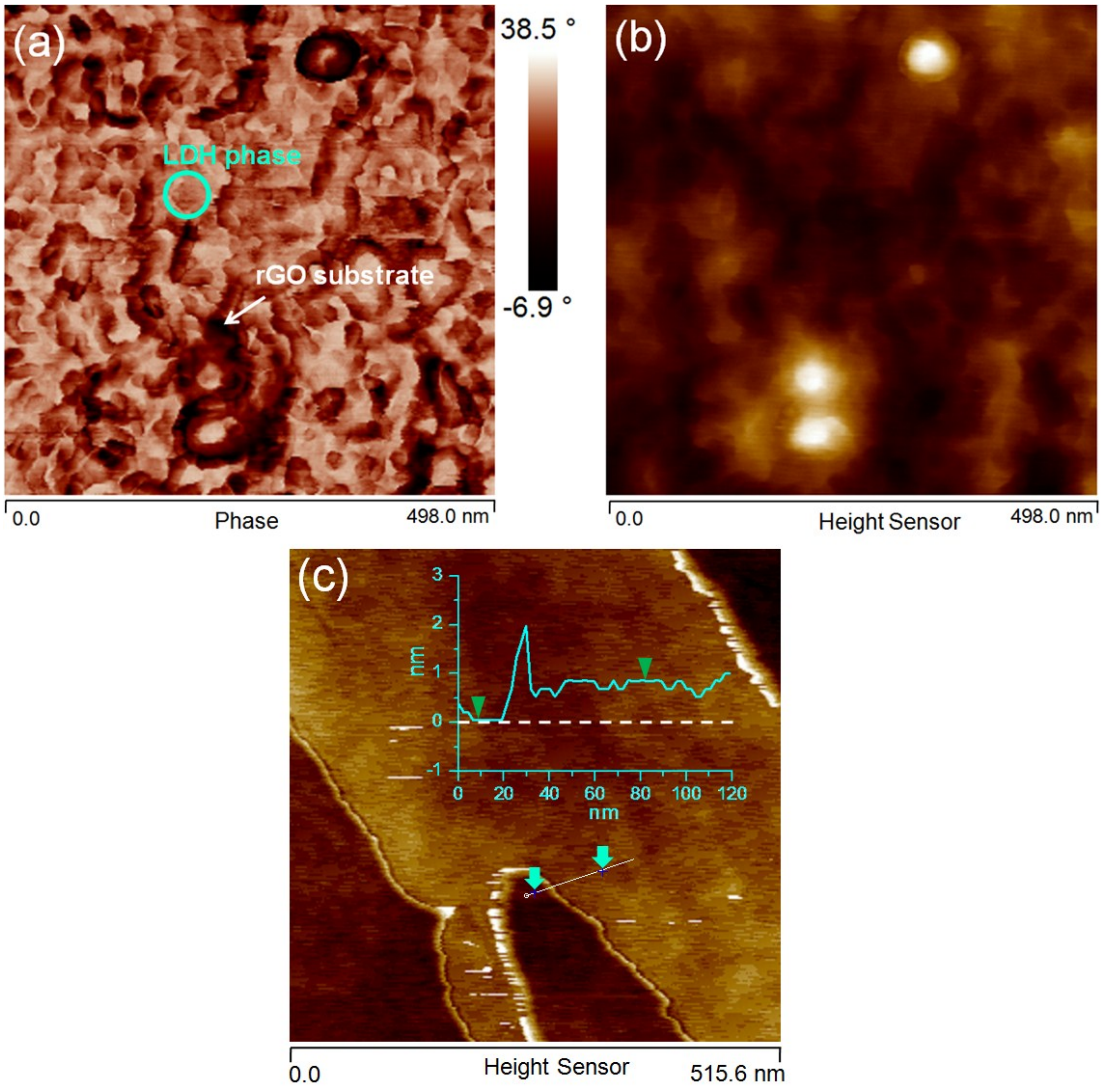

Figure S3. Two-dimensional phase (a) and topography (b) AFM images of 1.0Cu-LDH/rGO and the topography image together with cross-section analysis of rGO layer derived from 1.0Cu-LDH/rGO after treatment with 2 M HCl for 2 days (c).

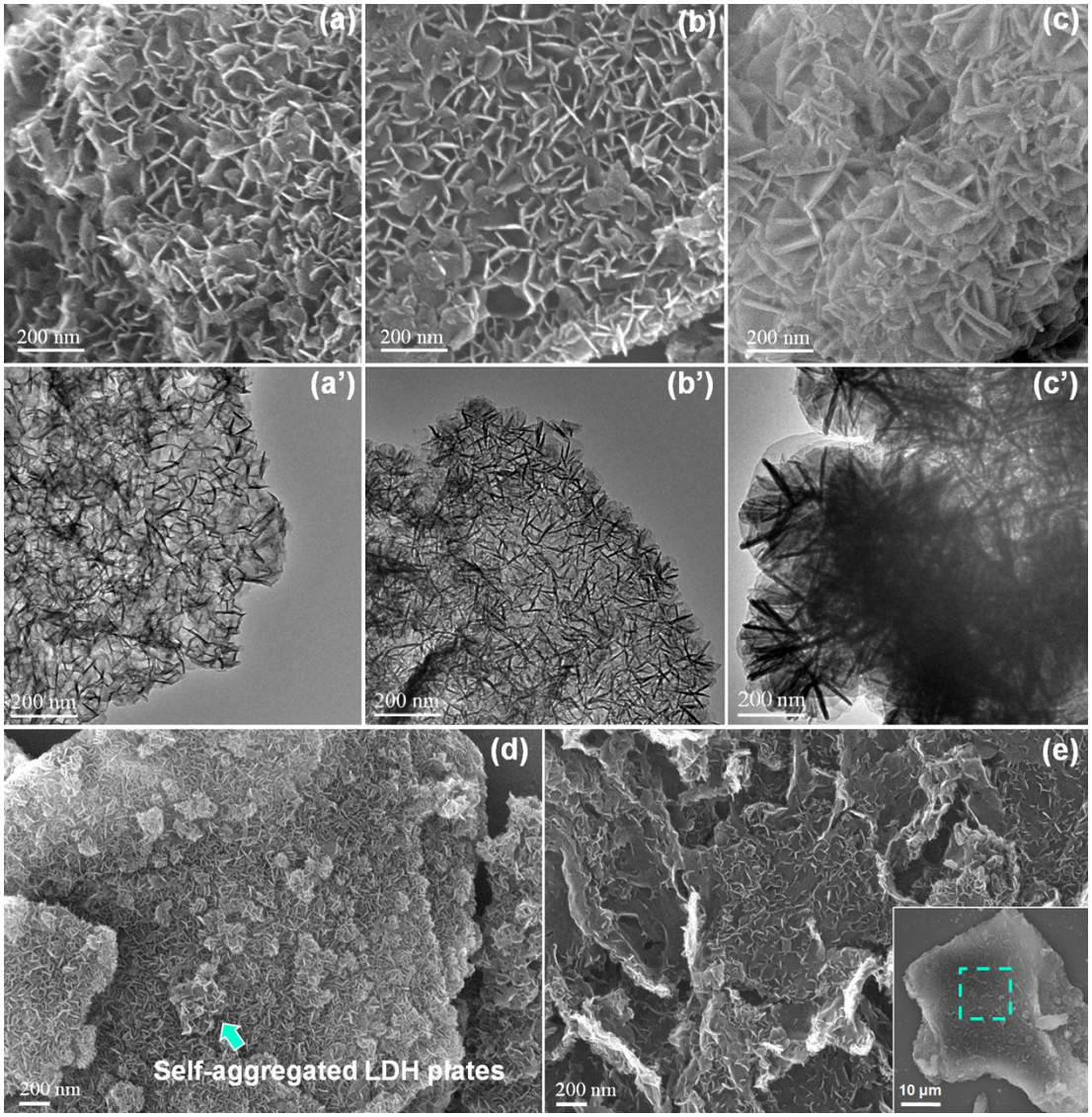

Figure S4. SEM (a-e) and TEM (a'-c') images of 0.5Cu-LDH/rGO (a, a'), 1.5Cu-LDH/rGO (b, b'), Cu-LDH (c, c'), 1.0Cu-LDH/rGO-25 (d) and 1.0Cu-LDH/rGO-100 (e).

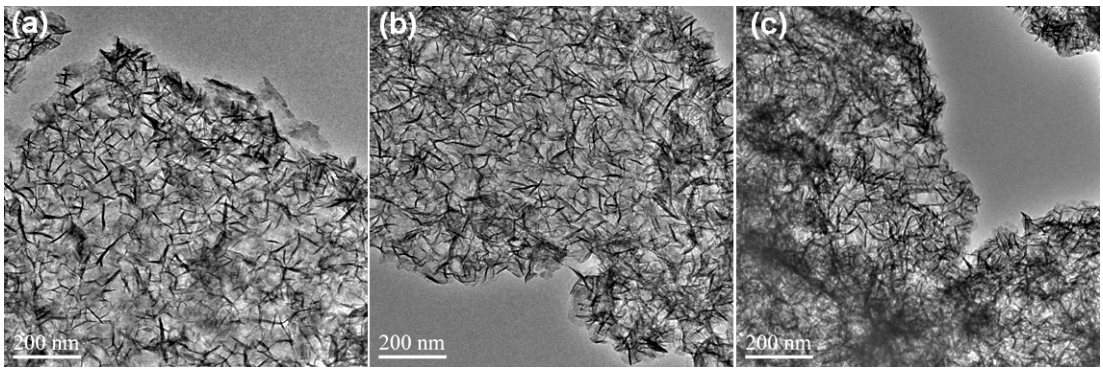

Figure S5. TEM images of Co_3Al-LDH/rGO (a), Co_2Ni_1Al-LDH/rGO (b), and $Cu_1Co_1Mg_1Al$-LDH/rGO (c) nanohybrids prepared by a green aqueous-phase coprecipitation strategy.

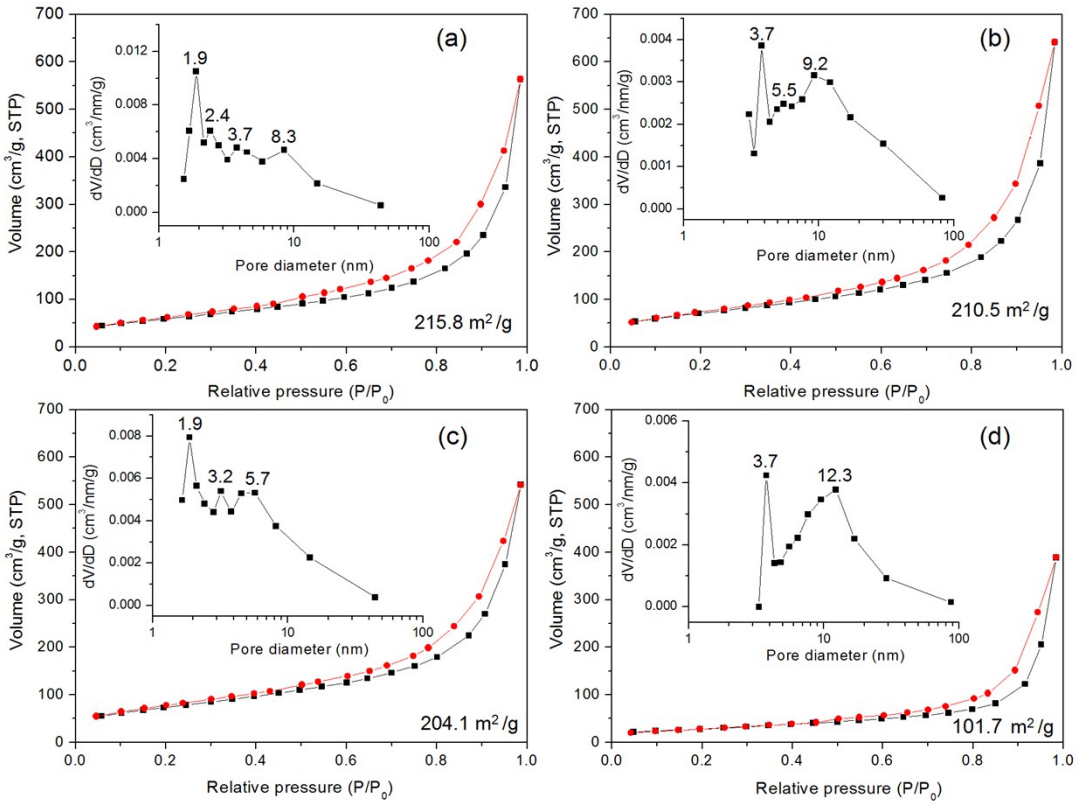

Figure S6. N_2 adsorption/desorption isotherms (inset: pore size distribution) of the hybrid catalysts 0.5Cu-LDH/rGO (a), 1.0 Cu-LDH/rGO (b), 1.5Cu-LDH/rGO (c) and Cu-LDH (d).

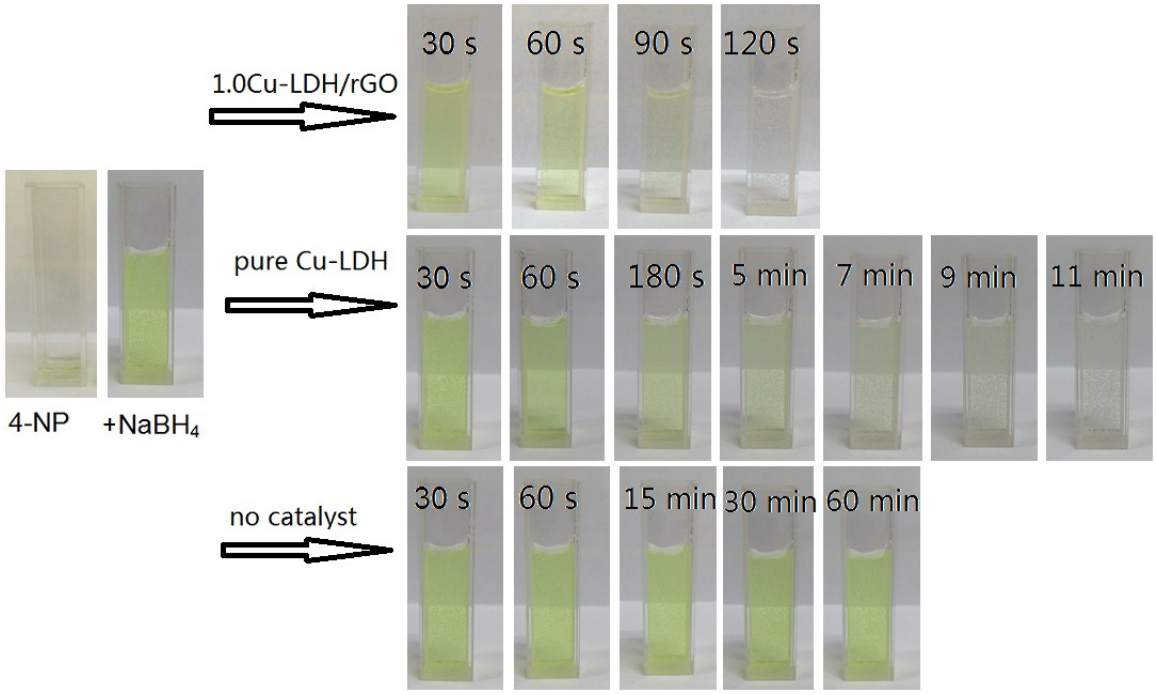

Figure S7. The time-dependent color changes of the 4-NP solutions during the reduction of 4-NP by $NaBH_4$ without catalyst and with 1.0Cu-LDH/rGO compared to pure Cu-LDH.

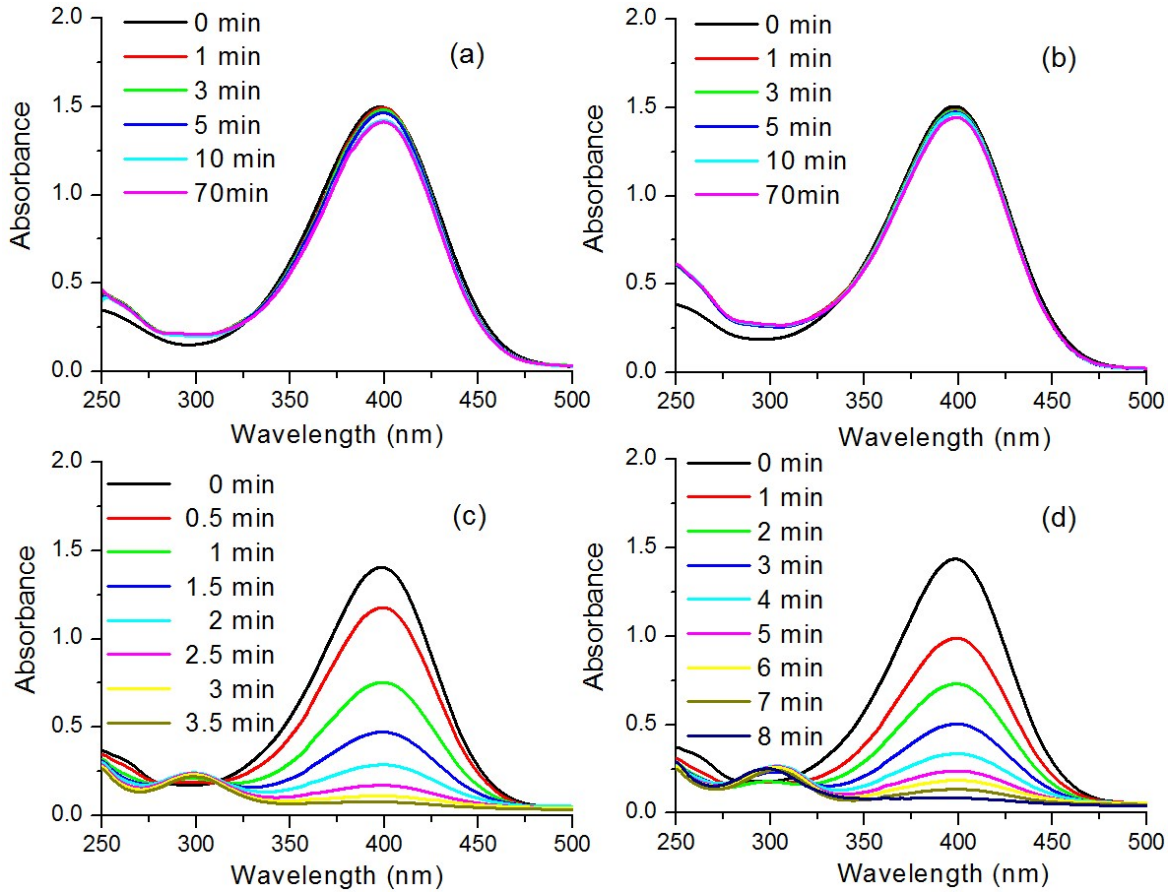

Figure S8. Time-dependent UV-vis absorption spectra of 4-NP solutions during the reduction of 4-NP by $NaBH_4$ with MgAl-LDH (a), GO (b), 1.0Cu-LDH/rGO-25 (c) and 1.0Cu-LDH/rGO-100 (d).

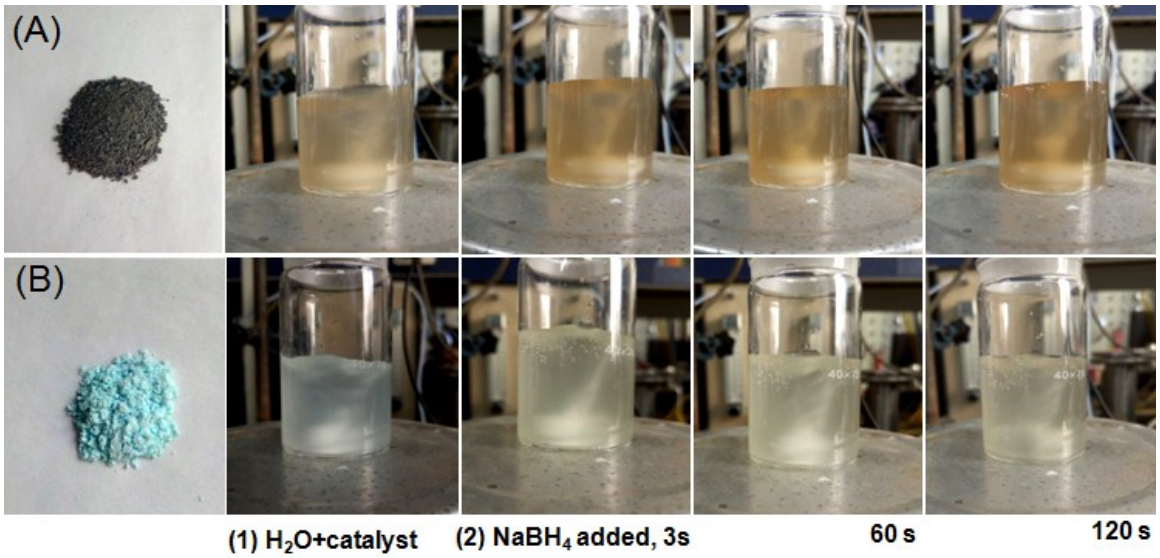

Figure S9. Photos of catalysts suspension (30 mL, 0.4 mg/mL) before and after addition of $NaBH_4$ (0.45 g) for 1.0Cu-LDH/rGO hybrid (A) and pure Cu-LDH (B).

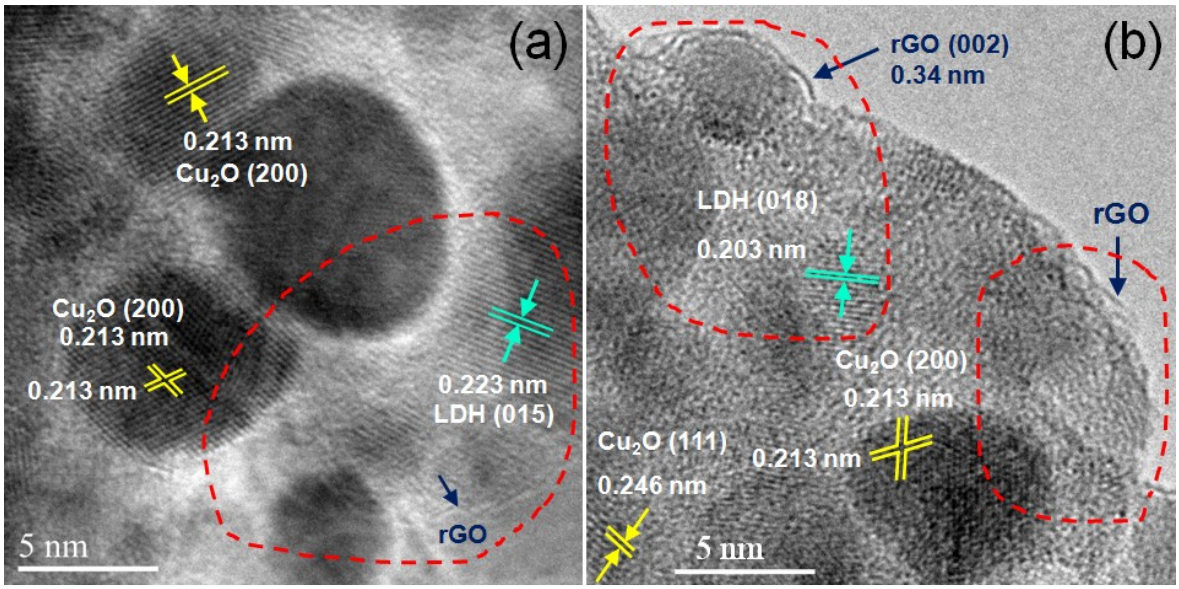

Figure S10. Evidence of strong three-phase synergistic effect among the *in situ* generated Cu_2O, *x*Cu-LDH and rGO substrate during the reduction reaction: HRTEM images (a and b) of 1.0Cu-LDH/rGO hybrid after treatment by $NaBH_4$ for 120 s.

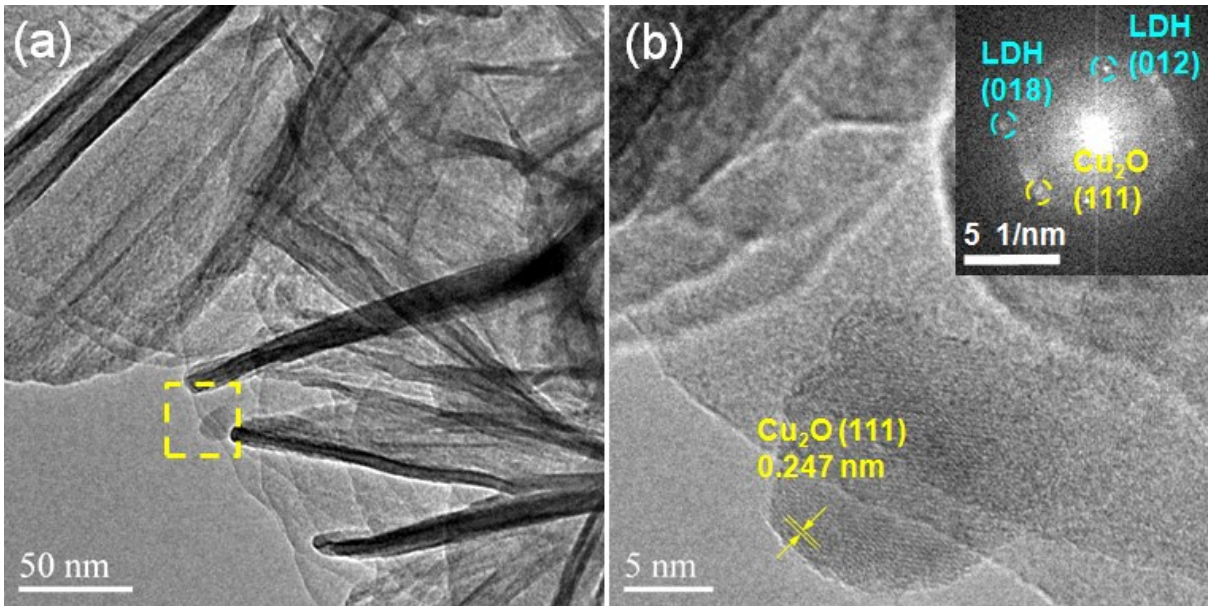

Figure S11. TEM (a) and HRTEM (b) images of pure Cu-LDH after treatment by $NaBH_4$ for 120 s (inset in (b), the SAED pattern).

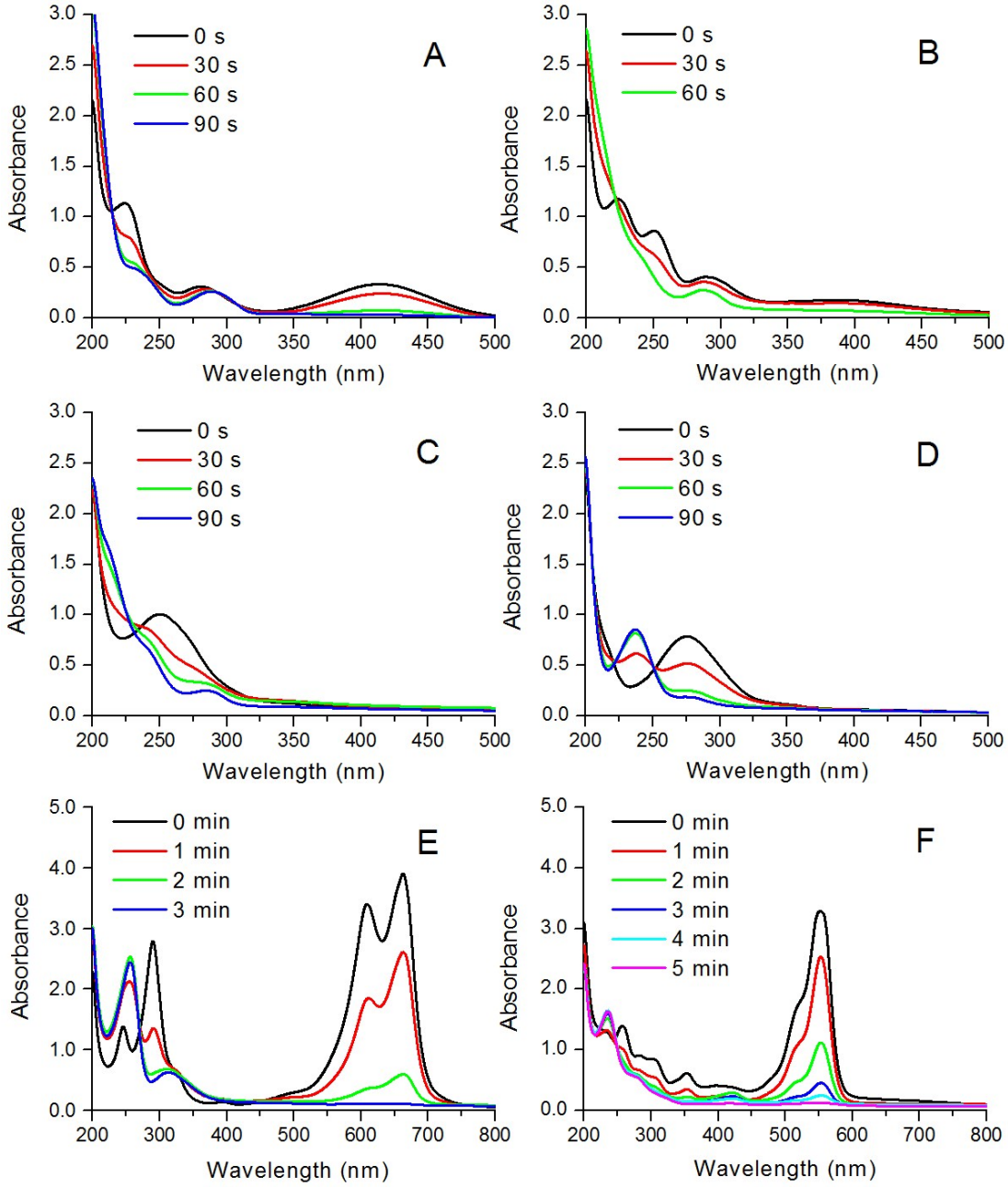

Figure S12. UV-vis absorption spectra of the reduction and degradation of diverse nitroarenes (A: 2-NP, B: 3-NP, C: 2,4-dinitrotoluene, and D: 4-nitrobenzaldehyde) and organic dyes (E: MB, and F: RhB) by $NaBH_4$ with the hybrid 1.0Cu-LDH/rGO.

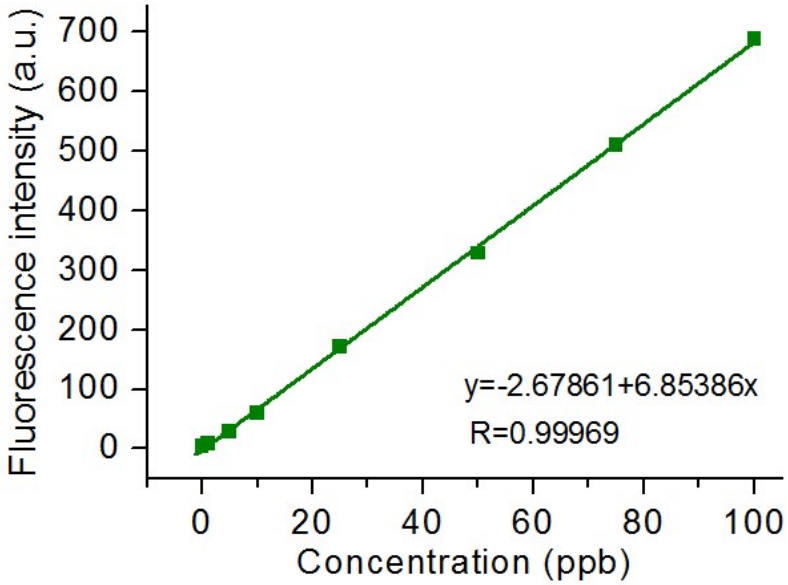

Figure S13. The correlated calibration curve of pyrene solution measured at 374 nm.

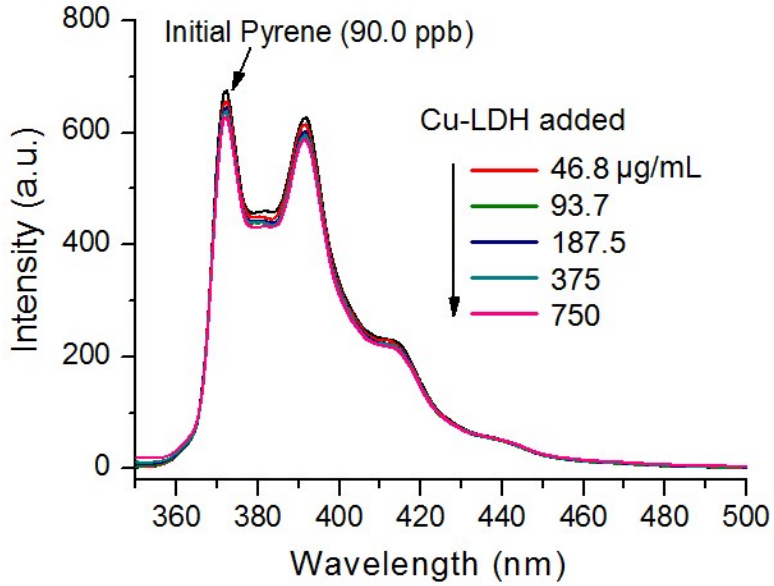

Figure S14. Fluorescence quenching of pyrene-contaminated water by adding Cu-LDH with varied concentrations (λ_{ex}=335 nm; initial concentration of pyrene: 90.0 ppb; adsorption time: 0.5 min).

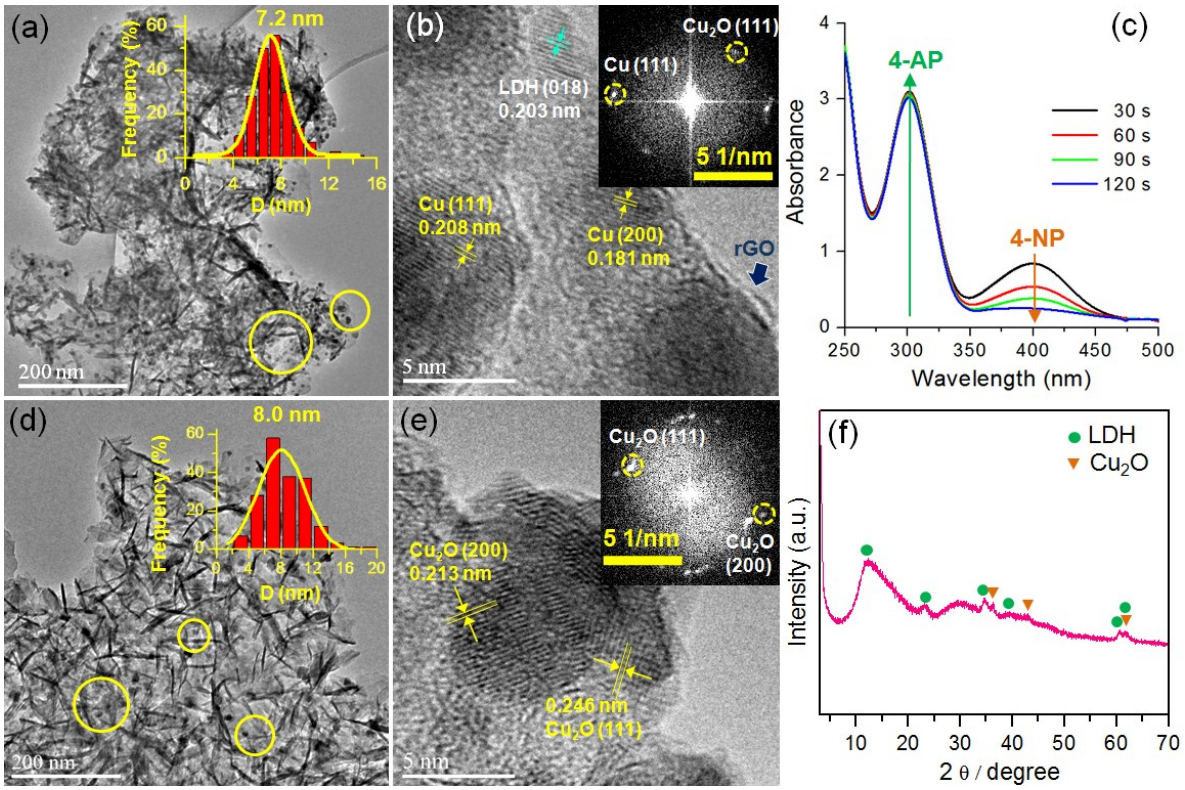

Figure S15. TEM (a, d), HRTEM (b, e), successive UV-vis absorption spectra (c) and XRD (f) of 1.0Cu-LDH/rGO recovered from 20th (a-c) and 10th (d-f) cycles of catalytic reduction of 4-NP (insets in (a, d), the particle size distributions on more than 200 particles; insets in (b, e), the SAED patterns).

Table S1. XRD parameters of the hybrids *x*Cu-LDH/rGO, Cu-LDH and MgAl-LDH.

Samples	d_{003}/nm	d_{110}/nm	*c*/nm [a]	*a*/nm [a]	D_{003}/nm [b]	D_{110}/nm [b]	I_{110}/I_{003} [c]
0.5Cu-LDH/rGO	0.7583	0.1525	2.27	0.3050	3.82	15.7	0.29
1.0Cu-LDH/rGO	0.7542	0.1526	2.26	0.3052	3.31	15.9	0.35
1.5Cu-LDH/rGO	0.7556	0.1529	2.27	0.3059	3.52	16.5	0.22
Cu-LDH	0.7690	0.1533	2.31	0.3067	8.30	22.0	0.16
MgAl-LDH	0.7815	0.1528	2.34	0.3057	7.52	21.2	0.18

[a] Based on hexagonal crystal system, $a = 2d_{110}$, $c = 3d_{003}$.

[b] Based on Scherrer equation. $D_{(hkl)} = k\lambda/(\beta\cos\theta)$ (k = 0.89, λ is the X-ray wavelength (0.1542 nm), θ is the diffraction angle and β is the full width at half-maximum (in radian)).

[c] The diffraction intensity ratio of (110) line to (003) line.

Table S2. The chemical compositions of the hybrids *x*Cu-LDH/rGO and Cu-LDH.

Catalysts	ICP		XPS	
	Cu/Mg/Al molar ratio	Cu (wt%)	Cu/Mg/Al molar ratio	Cu (wt%)
0.5Cu-LDH/rGO	0.50:2.47:1.00	8.36	0.50:4.98:3.65	5.69
1.0Cu-LDH/rGO	1.00:2.02:1.03	16.50	1.00:3.88:5.72	9.41
			1.00:1.55:5.49 [a]	12.61[a]
1.5Cu-LDH/rGO	1.50:1.45:1.02	22.38	1.50:3.58:7.61	13.13
Cu-LDH	1.00:1.98: 0.96	17.27	1.00:4.48:4.73	11.28

[a] 1.0Cu-LDH/rGO treated by $NaBH_4$ for 120 s.

Table S3. Catalyzing reduction and degradation of diverse nitroarenes and organic dyes over the hierarchical nanoarray-like hybrid 1.0Cu-LDH/rGO.

Entry	Substrate	Product	Time (min)	TOF (h^{-1})
1	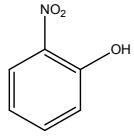	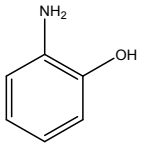	1.5	215.9
2	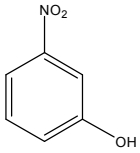	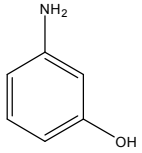	1.0	323.9
3	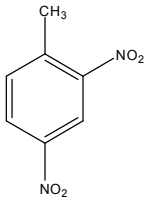	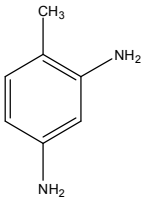	1.5	215.9
4	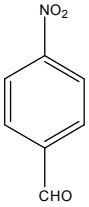	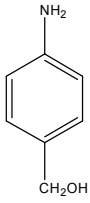	1.5	215.9
5	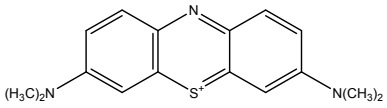	Aromatic ring-containing complex	3.0	108.0
6	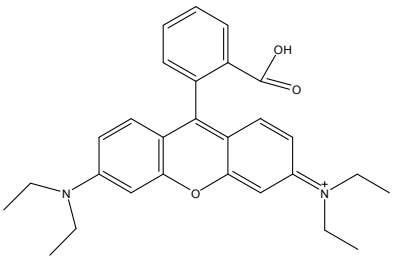	Aromatic ring-containing complex	5.0	64.8